

# 이중여자 유도형 풍력발전기 기반 풍력단지 의 계통 연계점 전압제어

## Voltage Control for a Wind Power Plant Based on the Available Reactive Current of a DFIG and Its Impacts on the Point of Interconnection

Yasir Usman\* · 김진호\*\* · Eduard Muljadi\*\*\* · 강용철†  
(Yasir Usman · Jinho Kim · Eduard Muljadi · Yong Cheol Kang)

**Abstract** - Wake effects cause wind turbine generators (WTGs) within a wind power plant (WPP) to produce different levels of active power and subsequent reactive power capabilities. Further, the impedance between a WTG and the point of interconnection (POI)—which depends on the distance between them—impacts the WPP's reactive power injection capability at the POI. This paper proposes a voltage control scheme for a WPP based on the available reactive current of the doubly-fed induction generators (DFIGs) and its impacts on the POI to improve the reactive power injection capability of the WPP. In this paper, a design strategy for modifying the gain of DFIG controller is suggested and the comprehensive properties of these control gains are investigated. In the proposed scheme, the WPP controller, which operates in a voltage control mode, sends the command signal to the DFIGs based on the voltage difference at the POI. The DFIG controllers, which operate in a voltage control mode, employ a proportional controller with a limiter. The gain of the proportional controller is adjusted depending on the available reactive current of the DFIG and the series impedance between the DFIG and the POI. The performance of the proposed scheme is validated for various disturbances such as a reactive load connection and grid fault using an EMTP-RV simulator. Simulation results demonstrate that the proposed scheme promptly recovers the POI voltage by injecting more reactive power after a disturbance than the conventional scheme.

**Key Words** : Doubly-fed induction generator, Voltage control, Wind power plant, Wake effect, Available reactive current, Point of interconnection

### 1. Introduction

Wind energy has become one of the fastest-growing sources of electricity in the world[1]. There has been growing interest in advanced control technologies for wind turbine generators (WTGs) or wind power plants (WPPs) to provide active and reactive power to power grids because of the increased share of wind energy on the electric grids in many countries[2]. Among the different wind energy conversion systems, doubly-fed induction generators (DFIGs) have been widely used because of their ability to meet control requirements without additional devices[3, 4]. Further,

DFIGs achieve variable-speed operation by using back-to-back power electronic convertors.

To maintain the bus voltages in the power grid within an allowable range, reactive power should be supplied by a generator or the reactive power compensating unit closest to the applicable bus. Recently, because of the increasing use of wind energy, transmission system operators in many countries have included in their grid codes additional technical requirements for the voltage control of the interconnection of large WPPs[5].

To comply with these requirements, hierarchical WPP control instead of distributed WPP control has been suggested[6-8]. Typically, the hierarchical structure consists of two levels of controllers: the WPP controller and the WTG controller. The latter maintains the terminal voltage of a WTG, whereas the former maintains the voltage at the point of interconnection (POI) of a WPP. The WPP and WTG controllers can be operated in either a voltage control mode or a reactive power control mode, depending on the control objective.

† Corresponding Author : Dept. of Electrical Engineering,  
Chonbuk National University, Korea  
E-mail : yckang@jbnu.ac.kr

\* Dept. of Electrical Engineering, Chonbuk National University, Korea

\*\* Dept. of Electrical Engineering, Chonbuk National University, Korea

\*\*\* National Renewable Energy Laboratory, USA.

Received : December 5, 2015; Accepted : December 13, 2015

Various research reports have been published on the hierarchical voltage control of a WPP[7-11]. In[7-9], a reactive power control mode was used for both WPP and WTG controllers. In[7], the WPP controller sends a reactive power reference signal proportional to its reactive power capability to each WTG. In[8], an optimization algorithm was suggested that uses the primal-dual predictor corrector interior point method to compute the reactive power reference for each WTG. A WPP controller was suggested that allocates a reactive current to each WTG based upon the average generated power of the WTG in[9].

A voltage control mode was used for both WPP and WTG controllers in[10, 11]. In[10], a WPP controller used the reactive power to voltage (Q-V) characteristic of a WPP to generate the voltage reference signal for each WTG. In contrast, the Q-V characteristic of a DFIG was used in the WTG controller in[11]. This scheme is capable of providing better performance in terms of voltage support than that described in[10]. However, these conventional schemes use the fixed Q-V characteristic based on the rated power irrespective of the reactive power capability, and thus their available reactive power is unable to be fully injected.

This paper proposes a voltage control scheme for a DFIG-based WPP. In the proposed scheme, a strategy that modifies the gain of the DFIG controller is developed to improve the reactive power injection capability of a WPP for a disturbance to secure the voltage stability of the power system. To achieve this, the WPP controller, which operates in a voltage control mode, sends the command signal to the DFIGs based on the voltage difference at the POI. The DFIG controllers, which operate in a voltage control mode, employ the reactive current to voltage (I<sub>q</sub>-V) characteristic determined by considering the available reactive current of a DFIG and the series impedance between the DFIG and the POI. The performance of the proposed scheme is validated for various disturbances such as the reactive load connection and grid fault using an EMTP-RV simulator.

## 2. Proposed Voltage Control Scheme for a DFIG-Based WPP

The proposed WPP voltage control scheme aims to improve the reactive power injection capability of a WPP by differentiating the contribution of DFIG<sup>i</sup>. To achieve this objective, the proposed scheme employs a hierarchical control scheme by using the WPP controller and DFIG controller. The following subsections describe the features of these two controllers.

### 2.1 WPP Controller

Fig. 1 shows the configuration of the WPP controller used in the proposed scheme. To maintain the POI voltage as the POI voltage set point,  $u_{ref}$ , the WPP controller operates in a voltage control mode and dispatches the voltage set point,  $\Delta u_{ref}^i$  to each DFIG. The WPP controller compares  $u_{ref}$  to the measured POI voltage,  $u_{POI}$ , and calculates the voltage error,  $u_{error}$ . The WPP controller determines  $\Delta u_{ref}^i$  which is the same for all DFIGs, using a proportional-integral controller. In this paper, the WPP controller sends  $\Delta u_{ref}^i$  to each DFIG every 100 ms using a hold function.

### 2.2 DFIG Controller

To ensure the voltage stability, WPPs should inject reactive power to support the voltage at the POI in the case of severe and small disturbances. To achieve this, the proposed scheme differentiates the contribution of DFIG<sup>i</sup> so that a DFIG that has a higher gain injects more reactive power than a DFIG that has a smaller gain. To do this, the I<sub>q</sub>-V gain of a DFIG is determined based on two factors: the available reactive current of DFIG<sup>i</sup> and the series impedance between DFIG<sup>i</sup> and the POI. The I<sub>q</sub>-V gain of DFIG<sup>i</sup> is set to be proportional to the former and inversely proportional to the latter. Thus, the proposed scheme can support the POI voltage more than the conventional scheme [11] by injecting more reactive power to the power grid.

Fig. 2 shows the rotor-side convertor (RSC) controller in the proposed scheme. The RSC controller, which also

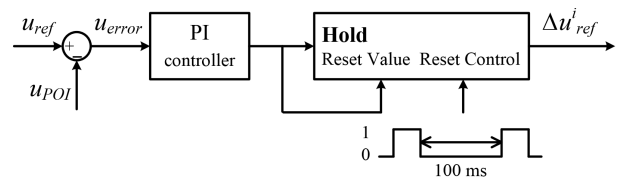


Fig. 1 WPP controller

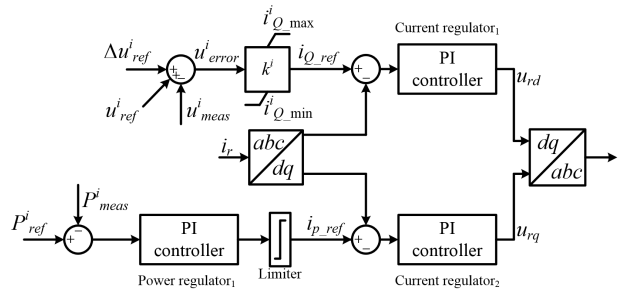


Fig. 2 RSC controller of DFIG<sup>i</sup>

operates in a voltage control mode, adjusts the reactive power injection at the DFIG terminal by changing the  $I_Q$ -V gain according to the operating conditions. The RSC controller receives  $\Delta u_{ref}^i$  from the WPP controller, and  $\Delta u_{ref}^i$  is added to the difference between the voltage set point of DFIG<sup>i</sup>,  $u_{ref}^i$ , and the measured voltage at the DFIG terminal,  $u_{meas}^i$ , to obtain the voltage error,  $u_{error}^i$ .  $u_{error}^i$  is then multiplied by the  $I_Q$ -V gain,  $k^i$ , to generate the reactive current reference,  $i_{Q,ref}^i$ .

### 2.2.1 Available Reactive Current of a DFIG

Fig. 3 shows the reactive current capability curve of the RSC controller. This curve can be obtained by using equation (1).

$$\begin{aligned} i_{Q,max}^i &= \sqrt{I_{rated}^2 - i_p^2} \\ i_{Q,min}^i &= -\sqrt{I_{rated}^2 - i_p^2} \end{aligned} \quad (1)$$

where  $i_{Q,max}^i$  and  $i_{Q,min}^i$  are the maximum and minimum reactive currents of DFIG<sup>i</sup>, respectively, and they have the same magnitude.  $i_p$  and  $I_{rated}$  are the active and rated currents of DFIG<sup>i</sup>, respectively.

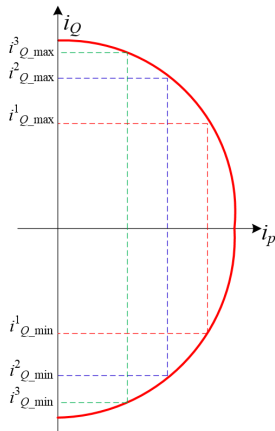


Fig. 3 Reactive current capability curve of RSC

Note that the reactive current capability of the RSC controller depends on the active current. Because of the wake effect, the wind speeds arriving at DFIG<sup>i</sup> are different, and thus each DFIG produces a different amount of the active current. Therefore, each DFIG will have different levels of reactive current capability. For example,  $i_{Q,max}^1$ ,  $i_{Q,min}^1$ ,  $i_{Q,max}^2$ ,  $i_{Q,min}^2$ ,  $i_{Q,max}^3$ , and  $i_{Q,min}^3$  in Fig. 3 are the maximum and minimum reactive currents of DFIG<sup>1</sup>, DFIG<sup>2</sup>, and DFIG<sup>3</sup>, respectively (see Fig. 7). For the

wind direction of 0 deg, DFIG<sup>1</sup> produces more active power than those of DFIG<sup>2</sup> and DFIG<sup>3</sup>, thereby  $i_{Q,max}^1$  is smaller than  $i_{Q,max}^2$  and  $i_{Q,max}^3$ .

### 2.2.2 $I_Q$ -V Characteristic of a DFIG

The  $I_Q$ -V characteristic of a DFIG consists of the  $I_Q$ -V gain and reactive current limits, as shown in Fig. 2. In the proposed scheme,  $k^i$  is defined as

$$k^i = \frac{i_{Q,max}^i - i_{Q,min}^i}{\Delta u^i} \quad (2)$$

$\Delta u^i$  in equation (2) is defined as

$$\Delta u^i = \Delta u \frac{|Z^i|}{\max(|Z^i|)} \quad (3)$$

where  $\Delta u$  is set to 0.2 p.u. in this paper, which is the maximum operating range in the grid code of [12], and  $|Z^i|$  is the magnitude of the series impedance between DFIG<sup>i</sup> and the POI.

Note that  $k^i$  is proportional to  $i_{Q,max}^i$ , and it is inversely proportional to  $\Delta u^i$ . To provide more understanding of (2), Fig. 4 shows an effect of  $i_{Q,max}^i$  on  $k^i$  if  $\Delta u^i$  is assumed to be a constant value of 0.2 p.u. Because DFIGs generate different amounts of active power, they have different  $i_{Q,max}^i$ . A DFIG that has a higher  $i_{Q,max}^i$  will have a higher gain. DFIGs reach the maximum values at  $\Delta u^i = \pm 0.1$  p.u. Because  $i_{Q,max}^1$  is smaller than  $i_{Q,max}^2$  and  $i_{Q,max}^3$ ,  $k^1$  is smaller than  $k^2$  and  $k^3$ .

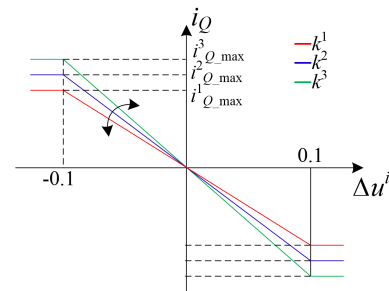


Fig. 4 Effect of  $i_{Q,max}^i$  on  $k^i$

In addition, Fig. 5 shows an effect of  $\Delta u^i$ —which is proportional to the series impedance between DFIG<sup>i</sup> and the POI—on  $k^i$  if  $i_{Q,max}^i$  are the same. A DFIG that is closer to the POI will have the smaller  $\Delta u^i$  and subsequently higher  $k^i$ , and thereby it injects more reactive current. Because DFIG<sup>3</sup> is closer to the POI than DFIG<sup>2</sup> and DFIG<sup>1</sup>,  $k^3$  is

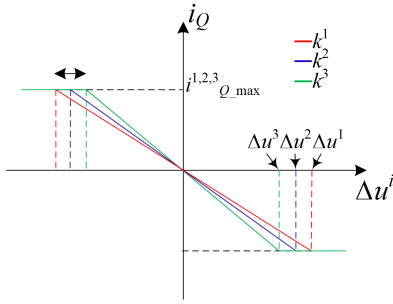


Fig. 5 Effect of  $\Delta u^i$  on  $k^i$

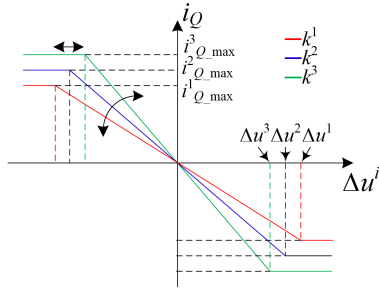


Fig. 6 Effect of  $i_{Q,max}^i$  and  $\Delta u^i$  on  $k^i$

larger than  $k^2$  and  $k^1$ . Note that DFIG<sup>3</sup> has a narrower linear region than DFIG<sup>2</sup> and DFIG<sup>1</sup>. This means that DFIG<sup>3</sup> can reach the reactive current limit with a smaller  $\Delta u^i$ .

Further, Fig. 6 shows the effect of both  $i_{Q,max}^i$  and  $\Delta u^i$  on  $k^i$ . The proposed scheme allows a DFIG with a higher  $i_{Q,max}^i$  and/or lower  $\Delta u^i$  to have a larger gain and narrower linear region so that it can inject more reactive power into a grid. Thus, a DFIG with a higher gain injects the maximum reactive current with a smaller  $\Delta u^i$ .

### 3. System Configuration

Fig. 7 shows a model system used to validate the performance of the proposed scheme using an EMTP-RV

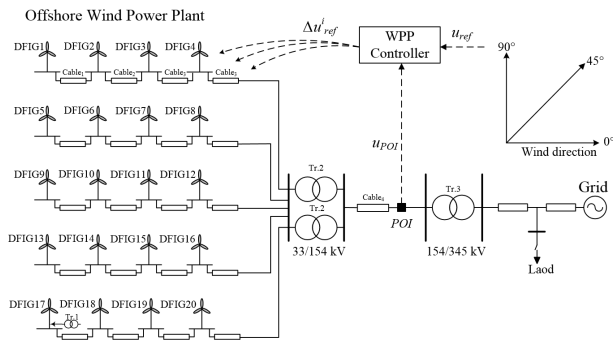


Fig. 7 Model system used in this paper

simulator. In the model system, a WPP consisting of 20 units of a 5-MW DFIG is connected to a power grid. In the WPP, the four DFIGs are connected to each feeder through 2.3/33-kV transformers. Five feeders are connected to the medium-voltage collector bus using 33-kV submarine cables. The collector bus is connected to the onshore 154/345-kV substation transformer through the two 33/154-kV step-up transformers and a 10-km-long submarine cable. The distance between the two neighboring DFIGs is set to 1 km. Table 1 shows parameters of transformers and cables in the model system. The WPP controller sends a reference signal to the DFIG controller at a rate of 0.1 s. Each DFIG controller samples the voltage and current at both stator side and rotor side at the sampling frequency of 10 kHz; the WPP controller also samples the POI voltage at the sampling frequency of 10 kHz; all the measured voltages and currents are passed through a second-order anti-aliasing low-pass filter with a cut-off frequency of 5 kHz (half the sampling frequency) to the WPP and DFIG controllers.

Table 1 Transformers and cables parameters in model system

	Tr.1(Y/Δ)	Tr.2(Δ/Y)	Tr.3(Y/Y)	
Capacity(MVA)	7.2	72	150	
Frequency(Hz)	60	60	60	
Turns Ratio(kV)	2.3/33	33/154	154/345	
% Impedance(p.u.)	0.07	0.07	0.07	
	Cable <sub>1</sub>	Cable <sub>2</sub>	Cable <sub>3</sub>	Cable <sub>4</sub>
Resistance(Ω/km)	0.344	0.130	0.064	0.056
Reactance(Ω/km)	0.172	0.172	0.132	0.151
Capacitance(μF/km)	0.117	0.160	0.209	0.141
Rated Voltage(kV)	33	33	33	154
Cross-Section Area(mm <sup>2</sup> )	70	185	400	500

As wind flows through a WPP, upstream WTGs influence the wind speed at the downstream WTGs. This is called the wake effect. In this paper, the wind speed in the wake for each WTG was calculated by using equation (4), as suggested in[13].

$$v_j = v_{j0} \sqrt{\sum_{\substack{k=1 \\ k \neq j}}^n \beta_k (v_{wk}(x_{kj}) - v_{j0})^2} \quad (4)$$

where  $v_{j0}$  is the incoming wind speed at WTG<sub>j</sub> without any shadowing,  $x_{kj}$  is the radial distance between WTG<sub>k</sub> and

WTG<sub>j</sub>,  $v_{wk}(x_{kj})$  is the speed of the wind approaching WTG<sub>j</sub> from the shadowing WTG<sub>k</sub>,  $b_k$  is the ratio of the area of WTG<sub>j</sub> under the shadow of WTG<sub>k</sub> to its total area, and  $n$  is the total number of WTGs.

#### 4. Case Studies

This section describes our investigation of the performance of the proposed control scheme for small and large disturbances under different wind conditions and short-circuit ratios (SCRs). Table 2 shows the wind speed of all DFIGs used for three cases. In each case, the proposed scheme was compared to the conventional scheme in [11], which uses the fixed Q-V gain at the DFIG level.

**Table 2** Wind speeds of all DFIGs (m/s)

For Cases 1 & 3 with 10 m/s, Wind Direction of 0°				For Case 2 with 12 m/s, Wind Direction of 45°			
Col.1	Col.2	Col.3	Col.4	Col.1	Col.2	Col.3	Col.4
10.00	7.75	7.37	7.26	12.00	9.83	9.61	9.55
10.00	7.75	7.37	7.26	12.00	9.83	9.61	9.55
10.00	7.75	7.37	7.26	12.00	9.83	9.61	9.61
10.00	7.75	7.37	7.26	12.00	9.83	9.83	9.83
10.00	7.75	7.37	7.26	12.00	12.00	12.00	12.00

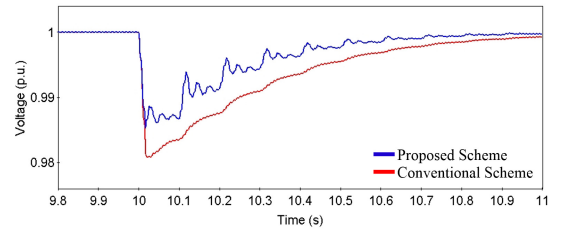
##### 4.1 For the Reactive Load Connection

In this subsection, to describe the effect of the proposed scheme on the voltage recovery at the POI, the performance of the proposed scheme is investigated for a reactive load connection.

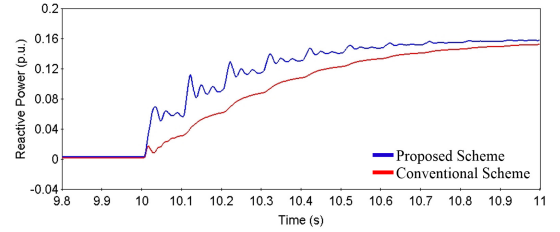
##### 4.1.1 Case 1: 60-MVar Load Connection at 10 s with Free Wind Speed of 10 m/s at 0° and SCR of 4

Fig. 8 shows the results for Case 1. As shown in Fig. 8(a), the proposed scheme shows the POI voltage recovery to the nominal value faster than the conventional scheme. This is because the proposed scheme supplies more reactive power to the grid than the conventional scheme after the reactive load connection (see Fig. 8(b)).

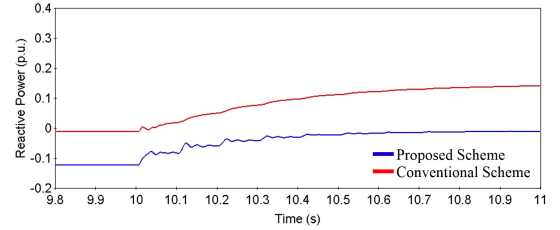
Figs. 8(c) and 8(d) show the reactive power from DFIG<sup>1</sup> and DFIG<sup>4</sup>, respectively. The proposed scheme modifies  $k^j$  based on  $i_{Q,max}$  and  $\Delta u^j$  of DFIG<sup>j</sup>. In the proposed scheme,  $k^1$ ,  $k^2$ ,  $k^3$ , and  $k^4$  prior to a disturbance were set to 9.83, 13.36, 17.32 and 23.33, respectively (see Fig. 8(e)), whereas in the conventional scheme, the gains for all DFIGs were set



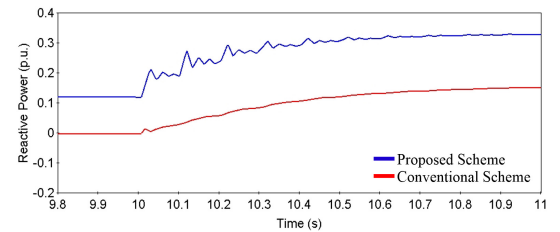
(a) Voltage at the POI



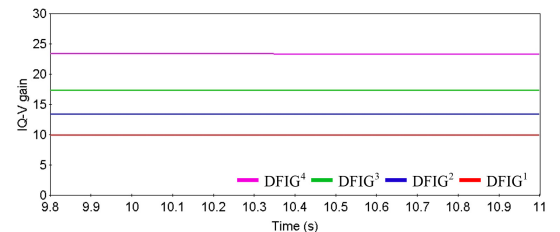
(b) Reactive power injection to the POI



(c) Reactive power from DFIG<sup>1</sup>



(d) Reactive power from DFIG<sup>4</sup>



(e)  $k^1$ ,  $k^2$ ,  $k^3$ , and  $k^4$

**Fig. 8** Results for Case 1

to a fixed value of 6.60. Note that in this case,  $k^1$ ,  $k^2$ ,  $k^3$ , and  $k^4$  remain the same after a disturbance. This is because the terminal voltages are constant after a disturbance and thus their active power outputs remain the same.

In the proposed scheme, DFIG<sup>4</sup>, which is closest to the POI, injects more reactive power than it does in the conventional scheme, as shown in Fig. 8(d). This is because a larger gain is set for DFIG<sup>4</sup> because of the smaller  $\Delta u^i$  and higher  $i_{Q,max}^i$  than the others. In contrast, DFIG<sup>1</sup>, which is located farthest from the POI and thus has a smaller  $i_{Q,max}^i$ , injects less reactive power than it does in the conventional scheme after the load connection because of the small  $u^1_{error}$ .

The results indicate that the proposed scheme can recover the POI voltage to the nominal value faster than the conventional scheme for the reactive load connection by differentiating the reactive power injection capability of the DFIGs according to  $i_{Q,max}^i$  and  $\Delta u^i$ .

#### 4.2 Effect of the Reactive Current Capability of a WPP

The voltage supporting capability of a WPP depends on wind conditions. In this subsection, the performance of the proposed scheme is investigated for a grid fault in different wind conditions.

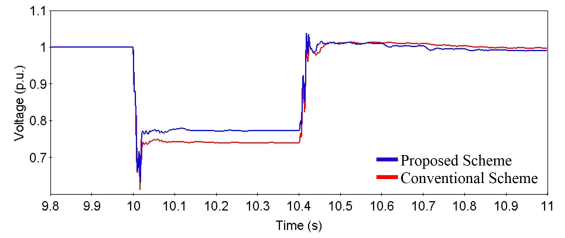
##### 4.2.1 Case 2: Grid Fault of 0.5 p.u. for 400 ms with a Free Wind Speed of 12 m/s at 45° and SCR of 6

Fig. 9 shows the results for Case 2. In the proposed scheme, during the fault period the POI voltage is supported higher than it is in the conventional scheme because the proposed scheme injects approximately twice than the conventional scheme (see Fig. 9(b)). As in Case 1, the proposed scheme modifies  $K^i$  depending on  $i_{Q,max}^i$  and  $\Delta u^i$ .  $K^1$ ,  $K^2$ ,  $K^3$ , and  $K^4$  prior to a disturbance were set to 8.86, 12.55, 16.33, and 22.03, respectively (see Fig. 9(e)). Thus, the proposed scheme can support the POI voltage at a higher level than the conventional scheme during the fault.

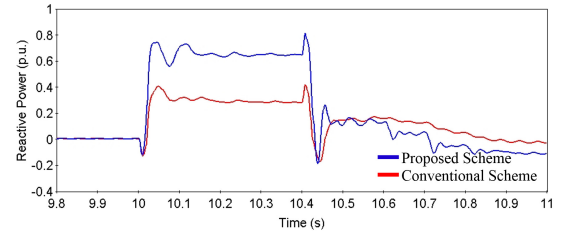
As shown in Figs. 9(c) and 9(d), in the proposed scheme, DFIG<sup>4</sup> injects more reactive power than DFIG<sup>1</sup> because of the higher  $i_{Q,max}^i$  and lower  $\Delta u^i$ . In addition, DFIG<sup>1</sup> in the proposed scheme injects reactive power two times that of the conventional scheme. In contrast, DFIG<sup>4</sup> in the proposed scheme injects the reactive power approximately three times that of the conventional scheme.

##### 4.2.2 Case 3: Grid Fault of 0.5 p.u. for 400 ms with a Free Wind Speed of 10 m/s at 0° and SCR of 6

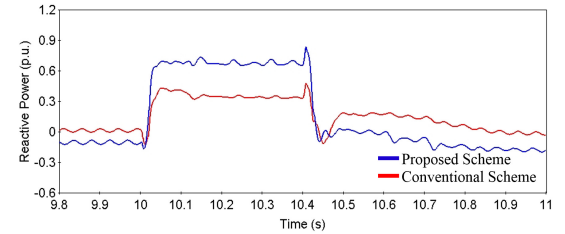
Fig. 10 shows the results for Case 3, which is identical



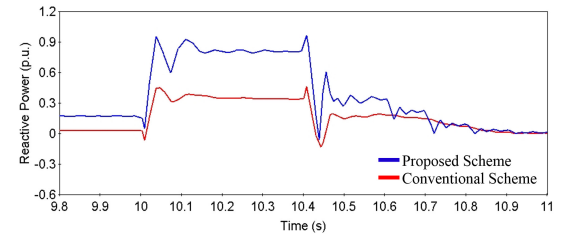
(a) Voltage at the POI



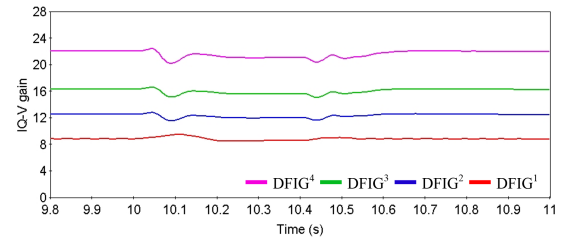
(b) Reactive power injection to the POI



(c) Reactive power from DFIG<sup>1</sup>



(d) Reactive power from DFIG<sup>4</sup>



(e)  $k^1$ ,  $k^2$ ,  $k^3$ , and  $k^4$

Fig. 9 Results for Case 2

to Case 2 except for the wind conditions. In this case, the wind speeds of the DFIGs are lower than they are in Case 2, and the resultant reactive power capability of the WPP is

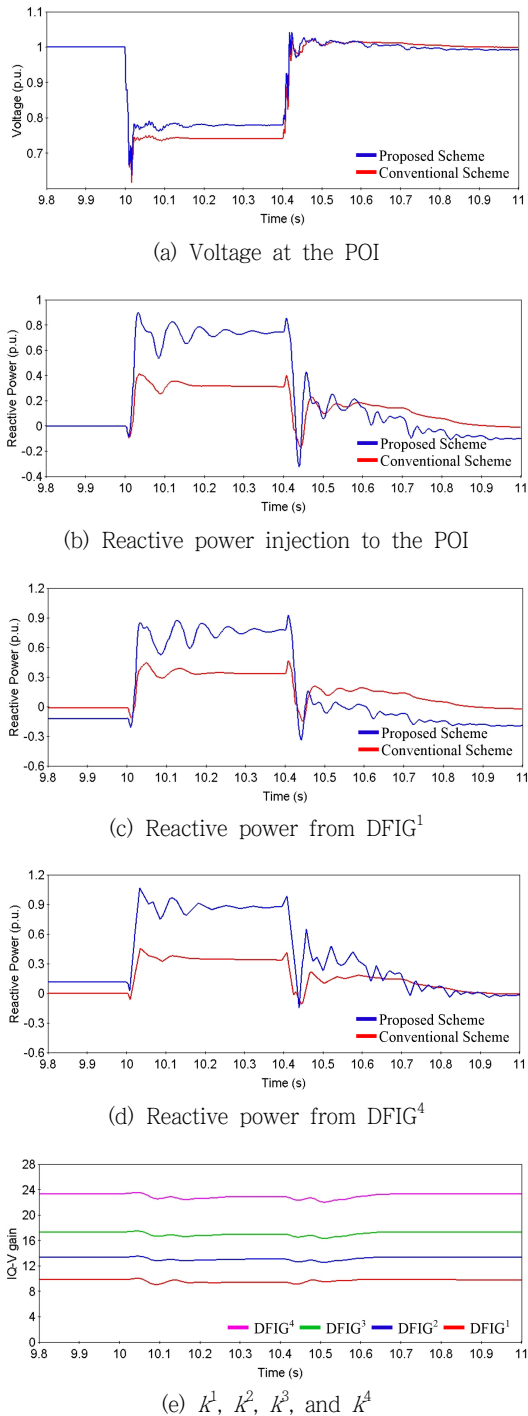


Fig. 10 Results for Case 3

larger than that of Case 2.

The POI voltage during the fault in the proposed scheme is higher than it is in the conventional scheme, because the proposed scheme injects more reactive power (see Fig. 10(b)). In addition, in this case, the proposed scheme injects more

reactive power into the grid than it does in Case 2. This is because  $K^1$ ,  $K^2$ ,  $K^3$ , and  $K^4$  prior to a disturbance were set to 9.83, 13.36, 17.32, and 23.35, respectively (see Fig. 10(e)), which are higher than they are in Case 2. As shown in Figs. 10(c) and 10(d), in the proposed scheme, DFIG<sup>4</sup> injects more reactive power than DFIG<sup>1</sup>, as in Case 2.

The results of the above two cases show that the proposed scheme supports the POI voltage at a higher level than the conventional scheme for grid faults by differentiating the gains of the DFIGs depending on  $\hat{i}_{Q,max}$  and  $\Delta u$ . Further, the voltage support capability of the proposed scheme can be enhanced for lower wind conditions.

### 5. Conclusion

This paper proposes a voltage control scheme for a DFIG-based WPP that can improve the voltage support capability of the WPP. To achieve this, the DFIG controllers use  $I_q$ -V gains determined by considering the reactive current capability and the distance between the DFIG and the POI. It differentiates the reactive power injection capability of the DFIGs in a WPP so that a DFIG that has higher reactive current capability and/or lower series impedance to the POI could inject more reactive power.

The simulation results clearly demonstrate that the proposed scheme can inject more reactive power than the conventional scheme in various wind conditions, thereby effectively supporting the POI voltages. In addition, the proposed scheme differentiates the control gains of a DFIG depending on the reactive current capability and its impacts on the POI, whereas the conventional scheme sets the same control gain irrespective of the reactive current capability.

### Acknowledgements

This work was supported by a National Research Foundation of Korea (NRF) grant funded by the Korean government (MSIP) (No. 2010-0028509).

### References

- [1] A. Zervos, "Renewables 2013 Global Status Report", Renewable Energy Policy Network for the 21st Century Paris, France, 2013.
- [2] J. Aho, A. Buckspan, J. Laks, P. Fleming, Y. Jeong, F. Dunne, M. Churchfield, L. Pao and K. Johnson, "A tutorial of wind turbine control for supporting grid

frequency through active power control”, In *Proceedings of the American Control Conference*, pp. 3120–3131, 2012.

- [3] M. Liserre, R. Cardenas, M. Molinas and J. Rodriguez, “Overview of multi-MW wind turbines and wind parks”, *IEEE Trans. Ind. Electron.*, vol. 4, pp. 1081–1095, 2011.
- [4] G. Byeon, I.K. Park and G. Jang, “Modeling and control of a doubly-fed induction generator (DFIG) wind power generation system for real-time simulations”, *J. Electr. Eng. Technol.*, vol. 5, pp. 61–69, 2010.
- [5] M. Tsili and S. Papathanassiou, “A review of grid code technical requirements for wind farms”, *IET Renew. Power Gen.*, vol. 3, pp. 308–332, 2009.
- [6] J. Martinez, P. Kjar, P. Rodriguez and R. Teodorescu, “Comparison of two voltage control strategies for a wind power plant”, In *Proceedings of the Power Systems Conference and Exposition*, pp. 1–9, 2011.
- [7] A.D. Hansen, P. Sørensen, F. Iov and F. Blaabjerg, “Centralised power control of wind farm with doubly fed induction generators”, *Renew. Energy*, vol. 31, pp. 935–951, 2006.
- [8] R. G. De Almeida, E. D. Castronuovo and J. Lopes, “Optimum generation control in wind parks when carrying out system operator requests”, *IEEE Trans. Power Syst.*, vol. 21, pp. 718–725, 2006.
- [9] E. Moursi, M. Shawky, G. Joos and C. Abbey, “A secondary voltage control strategy for transmission level interconnection of wind generation”, *IEEE Trans. Power Electron.*, vol. 23, pp. 1178–1190, 2008.
- [10] J. Fortmann and I. Erlich, “Use of a deadband in reactive power control requirements for wind turbines in european grid code”, In *Proceedings of the 11th International Workshop on Large-Scale Integration of Wind Power Into Power Systems*, Lisbon, Portugal, 2012.
- [11] J. Fortmann, M. Wilch, F. W. Koch and I. Erlich, “A novel centralised wind farm controller utilising voltage control capability of wind turbines”, In *Proceedings of the Power System Computation Conference*, 2008.
- [12] E.ON Netz GmbH, “*Grid Code High and Extra High Voltage*”, E.ON Netz GmbH, Germany, 2006.
- [13] F. Koch, G.M. resch, F. Shewarega, I. Erlich and U. Bachmann, “Consideration of Wind Farm Wake Effect in Power System Dynamic Simulation”, In *Proceedings of the Power Tech*, Russia, pp. 1–7, 2005.

## 저 자 소 개



**Yasir Usman** received his B.S. degree from COMSATS Institute of Information Technology, Pakistan in 2013. He is currently pursuing his M.S. degree at Chonbuk National University, Jeonju, Korea. His research interests include the

development of control methods for wind power plants.

Tel : 063-270-2391 Fax : 063-270-2394

E-mail : yasir\_usman48@jbnu.ac.kr



**Jinho Kim** received the B.S. and M.S. degrees from Chonbuk National University, Jeonju, Korea, in 2013 and 2015, respectively. His research interests include the development of integrated test bed for wind power plants.

Tel : 063-270-2391 Fax : 063-270-2394

E-mail : jkim@jbnu.ac.kr



**Eduard Muljadi** received the Ph.D. degree in electrical engineering from the University of Wisconsin at Madison, WI, USA. From 1988 to 1992, he was with California State University at Fresno. In June 1992, he joined the National Renewable Energy Laboratory, Golden, CO, USA. His current research interests include power electronics, and renewable energy applications.

Tel : +1-720-256-4110 Fax : +1-303-384-7060

E-mail : eduard.muljadi@nrel.gov



**Yong Cheol Kang** received the B.S., M.S., and Ph.D. degrees from Seoul National University, Seoul, Korea, in 1991, 1993, and 1997, respectively. Since 1999, he has been with Chonbuk National University, Jeonju, Korea, where he is currently a professor and director at the Wind energy Grid-Adaptive Technologies Research Center supported by the Ministry of Science, ICT, and Future Planning, Korea. His research interest includes the development of control systems for wind power plants.

Tel : 063-270-2391 Fax : 063-270-2394

E-mail : yckang@jbnu.ac.kr